



HAL
open science

Effect of the Wavy permeable Interface on Double Diffusive Natural Convection in a Partially Porous Cavity.

Razli Mehdaoui, Mohamed Elmir, Abdelkader Mojtabi

► **To cite this version:**

Razli Mehdaoui, Mohamed Elmir, Abdelkader Mojtabi. Effect of the Wavy permeable Interface on Double Diffusive Natural Convection in a Partially Porous Cavity.. The international journal of multiphysics., 2010, 4 (3), pp.217-231. 10.1260/1750-9548.4.3.217 . hal-03545802

HAL Id: hal-03545802

<https://hal.science/hal-03545802v1>

Submitted on 27 Jan 2022

HAL is a multi-disciplinary open access archive for the deposit and dissemination of scientific research documents, whether they are published or not. The documents may come from teaching and research institutions in France or abroad, or from public or private research centers.

L'archive ouverte pluridisciplinaire **HAL**, est destinée au dépôt et à la diffusion de documents scientifiques de niveau recherche, publiés ou non, émanant des établissements d'enseignement et de recherche français ou étrangers, des laboratoires publics ou privés.

Effect of the Wavy permeable Interface on Double Diffusive Natural Convection in a Partially Porous Cavity

Razli. Mehdaoui^{a,b}, Mohamed. Elmir^{a,b}, Abdelkader. Mojtabi^b

^aBechar University, PO Box 417, Bechar, Algeria,

^bIMFT, UPS, 118 route de Narbonne, 31062, Toulouse cedex, France

ramehd2002@yahoo.fr

mir0562@yahoo.fr

mojtabi@cict.fr

ABSTRACT

Two-dimensional, double diffusion, natural convection in a partially porous cavity saturated with a binary fluid is investigated numerically. Multiple motions are driven by the external temperature and concentration differences imposed across vertical walls. The wavy interface between fluid and porous layer is horizontal. The equations which describe the fluid flow and heat and mass transfer are described by the Navier-Stokes equations (fluid region), Darcy-Brinkman equation (porous region) and energy and mass equations. The finite element method was applied to solve the governing equations. The fluid flow and heat and mass transfer has been investigated for different values of the amplitude and the wave number of the interface and the buoyancy ratio. The results obtained in the form of isotherms, stream lines, isoconcentrations and the Nusselt and Sherwood numbers; show that the wavy interface has a significant effect on the flow and heat and mass transfer.

Keywords: Double diffusive; Wavy Interface; Porous; Darcy-Brinkman

1. INTRODUCTION

Double-diffusive natural convection in enclosures has been encountered in many engineering fields, such as oceanography, astrophysics, geology, biology, and chemical processes etc. The phenomenon of double-diffusive natural convection in an enclosure is as varied as the thermal and solutal boundary conditions, geometry and orientation of the enclosure. Judging from the number of potential engineering applications, the enclosure phenomena can be organized into three classes: (1) double diffusion in an horizontal layer with vertical temperature and concentration gradients [1–3]; (2) thermosolutal natural convection due to horizontal temperature and concentration gradients in vertical enclosures [2,4–16] and (3) sideways heating of an initially stratified fluid layer [17–19]. Other engineering systems, however, may be characterized by double-diffusive behavior driven by thermal and solutal buoyancies induced by discrete heat and mass sources. For example, possible non-uniformities in the release of buoyant element due to heat exchanger leakage in salt-gradient solar ponds [20], or crystal growth control [21] and in heat and moisture transport in building elements [22–26], also warrant the investigation of double-diffusive convection induced by discrete heat and mass sources. The literature survey illustrates the extensive works that have been carried out on square, rectangular shallow cavities with various wall boundary

conditions. An analytical and numerical study of natural convection heat and mass transfer through a vertical porous layer subjected to a concentration difference and a temperature difference in the horizontal direction has been studied by Trevisan and Bejan [27]. Many physical systems were modelled as a two-dimensional cavity with the vertical walls held at fixed but different temperatures or concentrations and the connecting horizontal walls considered as adiabatic or impermeable. Angirasa et al. [28] were reported a numerical study of combined heat and mass transfer by natural convection adjacent to vertical surfaces situated in fluid saturated porous media. Akbal and Baytas [29] have investigated a radioactive gas transfer depending on the decay of the gas, Schmidt and concentration Grashof numbers by natural convection in a fluid saturated porous medium. Merkin and Mahmood [30] have investigated a model for the convective flow in a fluid-saturated porous medium containing a reactive component. Goyeau et al. [31] have studied the double diffusive natural convection using Darcy—Brinkman formulation in a porous cavity with impermeable boundaries. Bahloul et al. [32] have investigated the double diffusive convection in a long vertical cavity heated from the below and imposed concentration gradient from the sides both analytically and numerically.

Double diffusive steady natural convection in a vertical stack of square enclosures, with heat and mass diffusive walls, was studied numerically by Costa [33]. Recently, researchers' studies on heat and mass transfer in composite systems constitute a fluid and porous medium saturated with the same fluid. Gobin et al. [34] have focused on the simulation of double diffusive convective flows in a binary fluid, confined in a vertical enclosure, divided into two vertical layers, one porous and the other fluid.

The combined heat and mass transfer rates for natural convection driven by the temperature and concentration gradients have been developed in a partially porous cavity by Singh et al. [35] and they showed that the degree of penetration of the fluid into porous region strongly depended upon the Darcy, thermal and solutal Rayleigh numbers. Mojtabi et al. [36] studied the Double diffusion natural convection in an enclosure filled with a liquid and subjected to differential heating and differential species concentration. Four models were developed to address the hydraulic effect of the upper lid on the rate of heat and mass transfer and on the flow structures.

The convective flows due to double-diffusion in a partially porous cavity saturated by a binary fluid have many applications, such as, soil pollution, thermal insulation, grain storage, dispersion of chemical contaminations through water saturated soil, storage of nuclear waste, fuel cells, heat removal from nuclear fuel debris in nuclear reactors, thermal energy storage system, solar collectors with a porous absorber. Another interesting application can be found in the accurate modeling of the boundary conditions at a fluid porous interface. Therefore, an understanding of the transport phenomena from a porous layer to a clear fluid layer and vice versa, and of the corresponding interface boundary conditions has become even more important. Most of the published studies on the natural convection in composite systems deal with cases in which the buoyancy forces are due to the variations of temperature only. As for as the boundary conditions, the use of the Brinkman correction allows to impose the continuity of the velocities and the tangential stresses to the fluid-porous interface. An alternative to the momentum transport description to the interface has been proposed by Ochoa-Tapia and Whitaker [37]. The authors established a boundary tangential stress-jump condition using the average volume technique. The choice of the interfacial condition was also analyzed recently by Goyeau et al. [38].

However, the studies of double diffusive convection in composite enclosures are very important in numerous scientific and industrial problems. A numerical study has been made of the double-diffusive natural convection in a rectangular fluid-saturated vertical porous

enclosure by Mamou et al. [39]. They showed that the effects of the buoyancy ratio to be rather significant on the flow pattern and heat and mass transfer. Bennacer et al. [40] performed a numerical analysis on the double diffusive, natural convection in a closed, vertical enclosure fitted with two symmetrical porous layers confining a fluid layer. Costa et al. [41] have used a control volume finite element method for simulating flows through a coupled fluid saturated porous and open domain.

Generally, the interface between the porous and fluid may not be flat or smooth everywhere. The shape of this interface may be from wavy form. For example, substrate of an agricultural greenhouse, thermal insulation. On the other hand, the bibliographical study shows that no work was found on the double-diffusive natural convection in partially porous cavity with a wavy interface (originality). The main object of the present study is to consider the effect of wavy shape horizontal interface on the double diffusive natural convection in a cavity. The equations which describe the fluid flow and heat and mass transfer are described by the Navier-Stokes equations (fluid region), Darcy- Brinkman equation (porous region) and energy and mass equations. The finite element method was applied to solve the governing equations. The fluid flow and heat and mass transfer has been investigated for different values of the amplitude and the wave number of the interface and the buoyancy ratio. The results obtained in the form of isotherms, stream lines, isoconcentrations and the Nusselt and Sherwood numbers; show that the wavy interface has a significant effect on the flow and heat and mass transfer.

2. MATHEMATICAL FORMULATION

The physical domain under investigation is a two-dimensional fluid-saturated Darcy–Brinkman partially porous cavity as illustrated in Figure 1. The square cavity is of side L and the Cartesian coordinates (x,y) . It is assumed that the third dimension of the cavity is large enough so that the fluid, heat and mass transports are two-dimensional. Gravity acts in the negative y -direction. the vertical surfaces are held at a constant temperature and concentration T_H, C_L , at $x = 0$ and T_C, C_R at $x = L$, respectively. The horizontal walls are adiabatic and impermeable. The horizontal wavy interface is considered to be permeable and fluid can flow from one layer to the other. In the present study, the porous layer covers the entire bottom wall of the cavity and its fluid/porous medium interface is placed at the horizontal mid plane of the cavity, i.e. at $y = L/2$. The fluid within the porous medium saturates the solid matrix and both are assumed to be in local thermodynamic equilibrium. The fluid flow is assumed to be laminar, incompressible, and the porous medium is assumed to be a homogenous and isotropic. Viscous dissipation and porous medium inertia are not considered, and the Soret and Dufour effects are neglected. Thermophysical properties are supposed constant. The fluid layer is filled with a Newtonian fluid of constant physical properties. According to Boussinesq’s approximation, the density is assumed to be a linear function of temperature and concentration as follow:

$$\rho = \rho_0 \left[1 - \beta_T (T - T_0) - \beta_C (C - C_0) \right]$$

$$\text{Where } \beta_T = - \frac{1}{\rho_0} \left(\frac{\partial \rho}{\partial T} \right)_{P,C} \text{ and } \beta_C = - \frac{1}{\rho_0} \left(\frac{\partial \rho}{\partial C} \right)_{P,T}$$

By employing the aforementioned assumptions into the macroscopic conservation equations of mass, momentum, energy and species and by combining the equations system for the two portions porous/fluid by a parameter:

$$\lambda = \begin{cases} 0 & \text{in the fluid region} \\ 1 & \text{in the porous region} \end{cases}$$

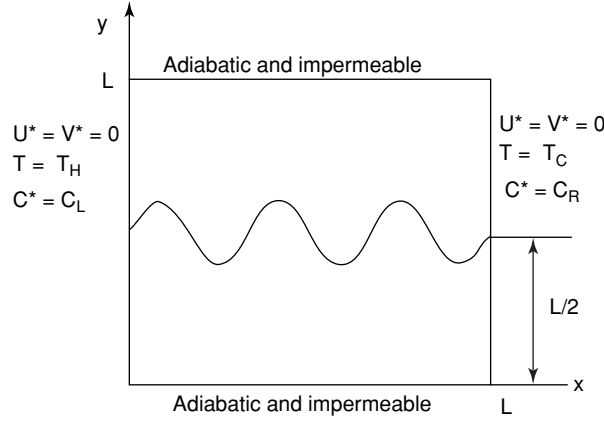


Figure 1 Physical model.

The nondimensional version of the governing system of transport equations are as follow:

$$\frac{\partial U}{\partial X} + \frac{\partial V}{\partial Y} = 0 \quad (1)$$

$$\left[\frac{\lambda}{\varepsilon} + (1-\lambda) \right] \frac{\partial U}{\partial \tau} + (1-\lambda) \left\{ U \frac{\partial U}{\partial X} + V \frac{\partial U}{\partial Y} \right\} = -[\lambda + (1-\lambda)] \frac{\partial P}{\partial X} + \text{Pr} \left(\frac{\partial^2 U}{\partial X^2} + \frac{\partial^2 U}{\partial Y^2} \right) - \lambda \frac{\text{Pr}}{\text{Da}} U \quad (2)$$

$$\left[\frac{\lambda}{\varepsilon} + (1-\lambda) \right] \frac{\partial V}{\partial \tau} + (1-\lambda) \left\{ U \frac{\partial V}{\partial X} + V \frac{\partial V}{\partial Y} \right\} = -[\lambda + (1-\lambda)] \frac{\partial P}{\partial Y} + \text{Pr} \left(\frac{\partial^2 V}{\partial X^2} + \frac{\partial^2 V}{\partial Y^2} \right) - \lambda \frac{\text{Pr}}{\text{Da}} V + \text{Ra Pr}(\text{T} + \text{NC}) \quad (3)$$

$$[\sigma\lambda + (1-\lambda)] \frac{\partial \theta}{\partial \tau} + U \frac{\partial \theta}{\partial X} + V \frac{\partial \theta}{\partial Y} = \left[\frac{k_{\text{eff}}}{k_f} \lambda + (1-\lambda) \right] \left(\frac{\partial^2 \theta}{\partial X^2} + \frac{\partial^2 \theta}{\partial Y^2} \right) \quad (4)$$

$$[\varepsilon\lambda + (1-\lambda)] \frac{\partial C}{\partial \tau} + U \frac{\partial C}{\partial X} + V \frac{\partial C}{\partial Y} = \left[\frac{D_{\text{eff}}}{D_f} \lambda + (1-\lambda) \right] \frac{1}{\text{Le}} \left(\frac{\partial^2 C}{\partial X^2} + \frac{\partial^2 C}{\partial Y^2} \right) \quad (5)$$

The nondimensional transport equations are obtained by adopting the following nondimensional quantities:

$$X, Y = \frac{1}{L}(X^*, Y^*); \quad U, V = \frac{L}{\alpha_f}(U^*, V^*),$$

$$\tau = \frac{\alpha_f}{L^2} \tau^*; \quad P = \frac{L^2}{\rho_f \alpha_f^2} P^*; \quad \theta = \frac{T^* - T_C}{T_H - T_E}, \quad C = \frac{C^* - C_R}{C_H - C_R} \quad (6)$$

In the above system, the following nondimensional parameters appear:

$$\text{Ra} = \frac{g\beta_T L^3 \Delta T}{(v\alpha)_f}; \quad \text{Pr} = (v/\alpha)_f; \quad \text{Da} = K/L^2$$

$$La = \alpha_f/D; N = \frac{\beta_c \Delta C}{\beta_f \Delta T}; \sigma = \frac{(\rho c_p)_p}{(\rho c_p)_f}$$

The initial conditions with $\tau = 0$ are:

$$U = V = \theta = C = 0$$

The nondimensional boundary conditions for Eqs. (1)-(5) are as follows:

$$\begin{aligned} \text{For } \tau > 0: \quad U = V = 0 \text{ and } \theta = C = 1 & \quad \text{at } X = 0, 0 \leq Y \leq 1 \\ U = V = \theta = C = 0 & \quad \text{at } X = 1, 0 \leq Y \leq 1 \\ \partial\theta/\partial Y = \partial C/\partial Y = U = V = 0 & \quad \text{at } Y = 0, 1 \text{ and } 0 \leq X \leq 1 \end{aligned}$$

At the wavy interface between the porous/fluid medium, the continuity conditions are as following:

$$\begin{aligned} U|_p = U|_f, V|_p = V|_f, P|_p = P|_f, \theta|_p = \theta|_f, \frac{\partial\theta}{\partial n}|_f = \frac{k_{eff}}{k_f} \frac{\partial\theta}{\partial n}|_p, \\ C|_p = C|_f, \frac{\partial C}{\partial n}|_f = \frac{D_{eff}}{D_f} \frac{\partial C}{\partial n}|_p \end{aligned}$$

The local and average Nusselt and Sherwood numbers are defined, respectively, as follows:

$$\begin{aligned} Nu_L = -\frac{\partial\theta}{\partial X}|_{X=1}; Sh_L = -\frac{\partial C}{\partial X}|_{X=1} \\ Nu_{avg} = \int_0^1 -\frac{\partial\theta}{\partial X} dY; Sh_{avg} = \int_0^1 -\frac{\partial C}{\partial X} dY \end{aligned}$$

3. NUMERICAL METHOD AND VALIDATION

Numerical results are obtained by solving the system of differential eqns (1)–(5), with appropriate boundary conditions, using the Galerkin finite-element method in order to ensure continuity of the convective and diffusive Fluxes, overall energy and momentum conservation. The two-dimensional spatial domain is divided into quadrangle elements (unstructured mesh) and a Lagrange-quadratic interpolation has been chosen. Accuracy tests were performed for the steady state results using five sets of uniform grids as shown in Table1.

Table1

Grid Sizes	Nu _{avg}	Sh _{avg}
22 × 22	1,705	1,702
32 × 32	1,765	1,758
42 × 42	1,763	1,756
52 × 52	1,763	1,756
62 × 62	1,763	1,756

The mesh is refined near the boundaries and we have adopted 1764 elements and the number of freedom degree is equal to 7225 (Figure.2). The grid selected for 42 × 42 as a

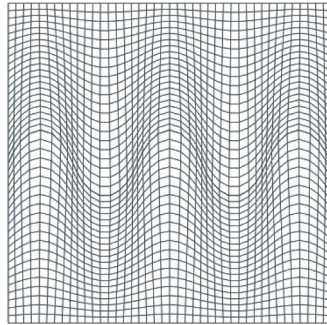


Figure 2 Mesh grid.

Table 2 Validation of the numerical code in the case of pure thermal convection ($N = 0$) for $Ra = 10^5$, $Pr = 0,71$, $k_r = 2$, $\varepsilon = 0,51$, $Da = 0,002$.

	Present study	Beckermann	S.B.Sathe et al
	Nu_{avg}	Nu_{avg}	Nu_{avg}
$S = 0,25$	3,19	3,4	3,6
$S = 0,5$	3,26	3,2	3,34
$S = 0,75$	3,008	3,101	2,9

trade off between numerical accuracy, stability and computational time. A nonlinear solver has been used and the nonlinear tolerance has been set to 10^{-6} .

Table 2 shows the comparison of Nu_{avg} for various values of the Width of porous region (S). The accuracy of the numerical code was checked in the case of Natural convection flow and heat transfer between a fluid layer and a porous layer inside a rectangular enclosure subject to a temperature difference in the vertical directional. The results concern mass transfer due to purely thermal natural convection ($N = 0$) for Darcy-Brinkman model. These results are in good agreement with those presented by Beckermann et al [42] and S.B.Sathe et al [43].

4. RESULT AND DISCUSSION

In the foregoing simulations, the main interest in this study is focused on the effect of the horizontal wavy interface (porous-fluid) on the structure of the fluid flow, and the heat and mass transfer for in the partially porous cavity. The following parameters are fixed:

$$Pr = 0,71, \varepsilon = 0,5, Le = 0,84, Ra = 10^5, Da = 10^{-4}, \frac{k_{eff}}{k_f} = 1, \frac{D_{eff}}{D_f} = 1$$

Figure 3 represents the distribution of the isoconcentrations, the streamline and, the isotherms for various values of dimensionless amplitude $A = 0; 0,05; 0,1; 0,15; 0,2$. The streamlines are organized in a convective cell of strong intensity of the flow circulation forces in the fluid region, while the flow fluid in the porous region is almost motionless; this distribution indicates clearly that the warm and solute enriched fluid flows along the hot vertical wall. It is observed that the phenomena of reversed transport occur along the cold vertical wall and the fluid flow in a clockwise circulation. The isotherms and isoconcentration lines are characterized by a thermal and mass stratification in the porous portion which is characterized by a weak thermal and mass gradient. In the center of the fluid

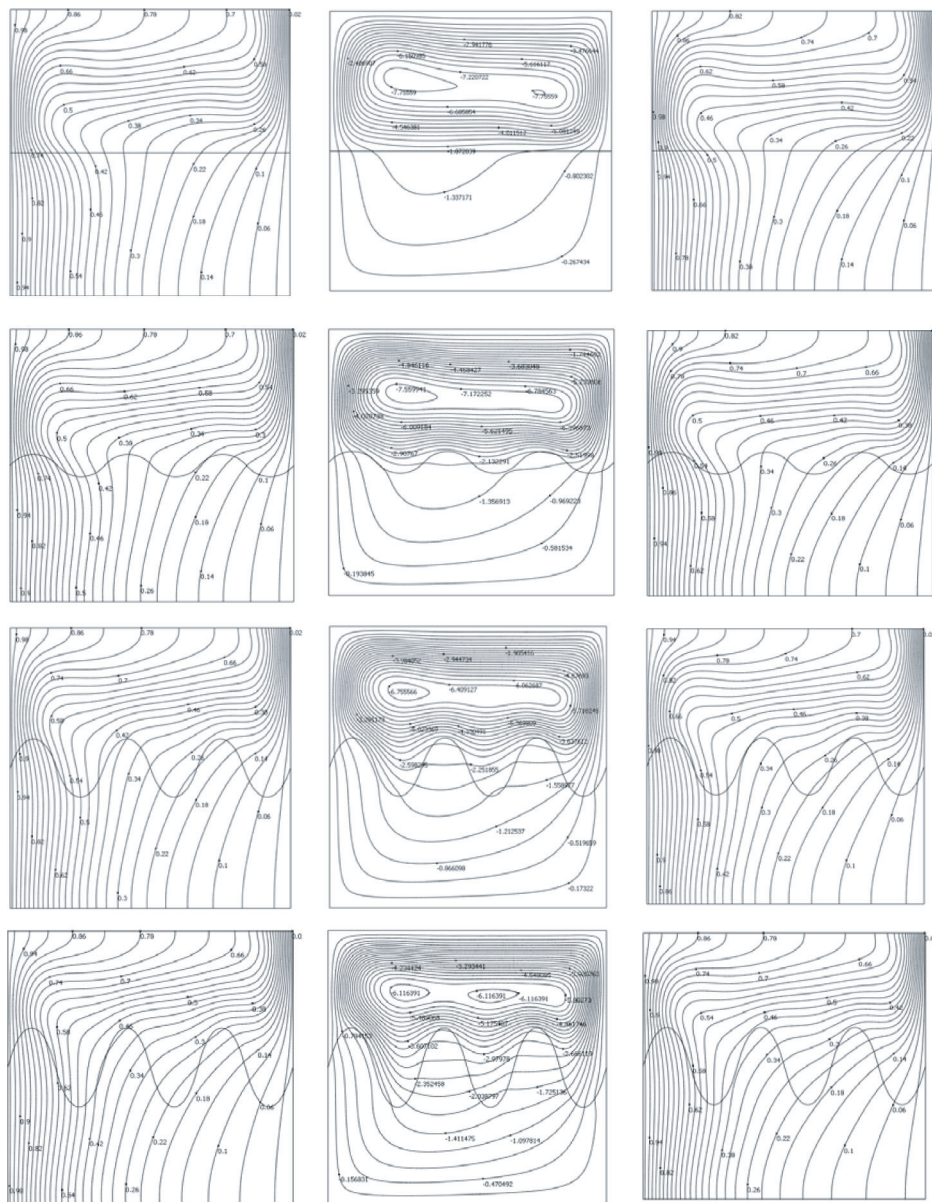


Figure 3 Isoconcentration lines, Streamlines and isotherms for $Ra = 10^5$; $N = 1$; $Da = 10^{-4}$; $Le = 0, 84$; $n = 3$; $Pr = 0,71$, $\epsilon = 0, 5$ and $A = 0, 0 - 0,05 - 0, 1 - 0, 15 - 0,2$.

layer these isotherms and isoconcentrations are perpendicular to the temperature gradient and concentration of the vertical walls. The structure of the distribution field proves that the flow intensity is more important in the fluid layer than in the porous one thus favoring a convective mode of flow in the fluid portion. It is observed that this intensity of circulation forces weakens with the increase in the adimensional amplitude A and the zone of the pseudo conductive flow widens.

Figure 4 represents the distribution of the isoconcentrations, the streamlines, and the isotherms for various values of the undulation number $n=1, 2, 3$ and 4 . The flow structure always arises in a convective cell characterized by a vortex which moves from the cold vertical wall towards the hot vertical one. The isoconcentrations and the isotherms are always

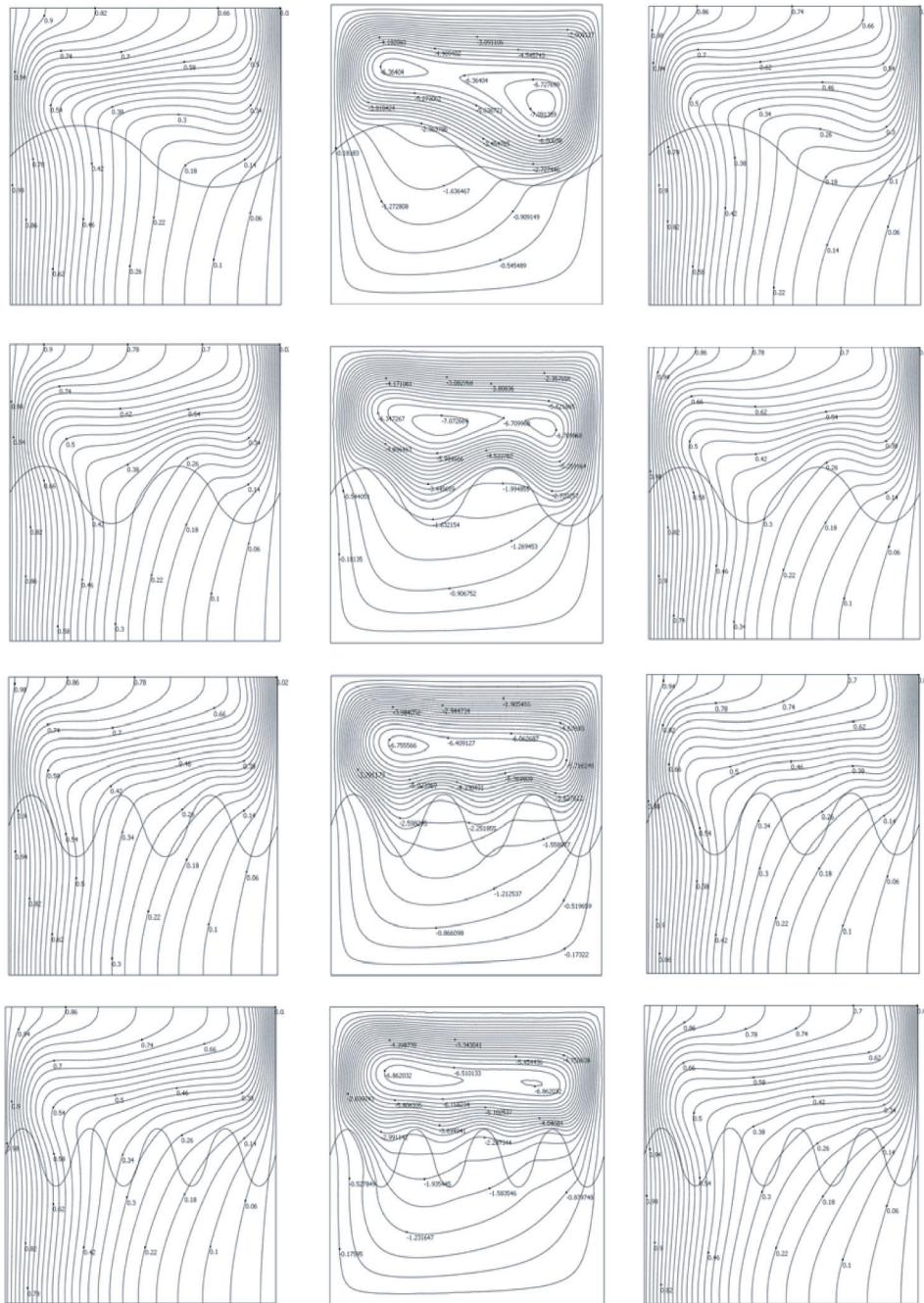


Figure 4 Isoconcentration lines, Streamlines and isotherms for $Ra = 10^5$; $N = 1$; $Da = 10^{-4}$; $Le = 0, 84$; $A = 0,1$; $Pr = 0,71$, $\varepsilon = 0,5$ and $n = 1, 2, 3, 4$.

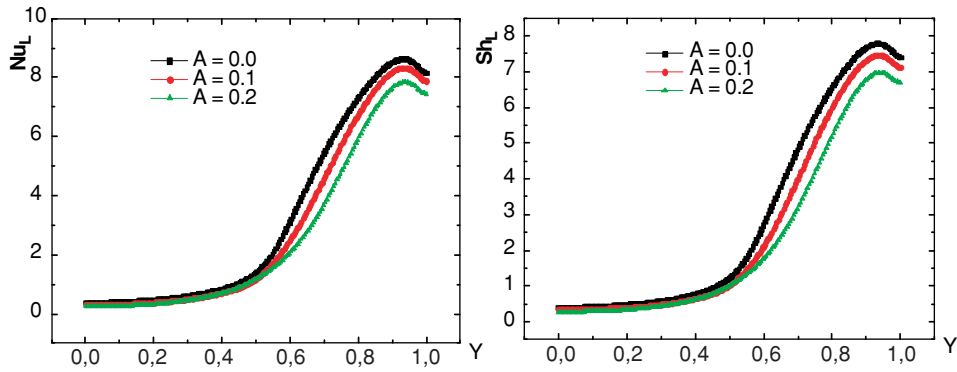


Figure 5 Local Nusselt number, and local Sherwood number for $Ra = 10^5$; $N = 1$; $Da = 10^{-4}$; $Le = 0.84$; $n = 2,5$; $\epsilon = 0,5$ at $X = 1$.

characterized by their thermal and mass stratifications in the porous zone. While in the fluid layer, the latter become almost parallel to the gravitation always favoring the convective mode flow at the centre of the fluid layer. With the increase in the undulation number n , the convective cell narrows more and more allowing to favored the conductive and diffusive mode flow in most of the cavity. One observes also the large temperature and concentration gradients located on the top part of the cavity. The effect of the undulation number also appears on the temperature values, as well as on the concentrations and stream functions.

Figure 5 represents the evolution of the local Nusselt and Sherwood numbers along the cold vertical wall, for various values of the adimensional amplitude $A=0; 0,1$ and $0,2$. These two numbers evolve in the same way and increase along the cold vertical wall. The figure shows that the increase in the value of the amplitude A does not have any influence on the variation of local Nusselt and Sherwood numbers in the porous layer, while a light variation on the values of two numbers is observed in the fluid layer with the amplitude variation.

Figure 6 represents the variation of the average Nusselt and the Sherwood numbers according to the value of the dimensionless amplitude A , on the cold vertical wall. The two

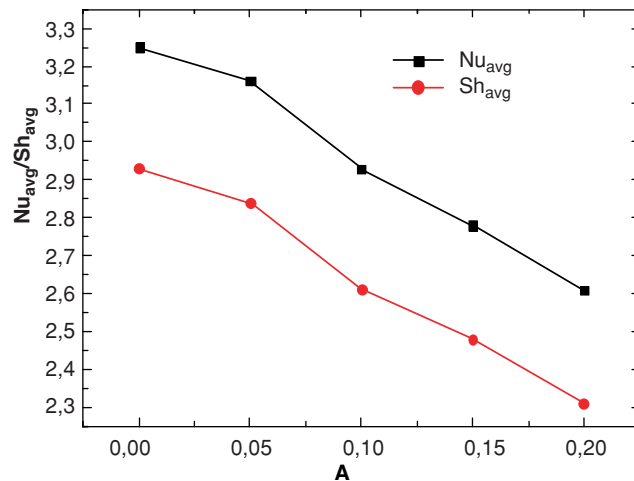


Figure 6 Average Nusselt and Sherwood number us function of A , for $Ra = 10^5$, $N = 1$, $Da = 10^{-4}$, $Le = 0.84$, $n = 3$, $\epsilon = 0,5$.

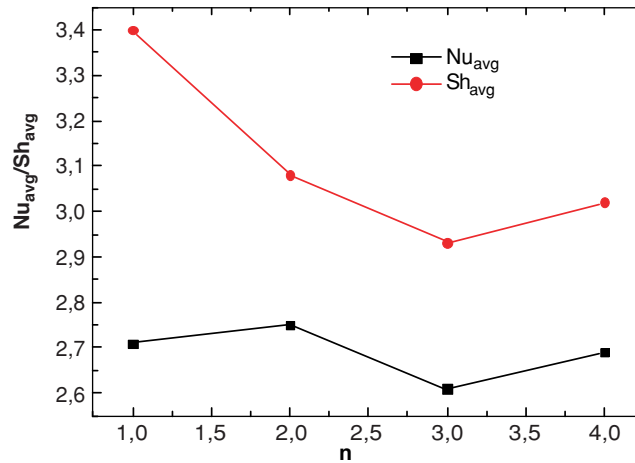


Figure 7 Average Nusselt and Sherwood number us function of n , for $Ra = 10^5$, $N = 1$, $Da = 10^{-5}$, $Le = 0.84$, $A = 0,1$, $\varepsilon = 0,5$.

numbers evolve almost linearly and in a decreasing way with the increase of the dimensionless amplitude A report. The value of A has a considerable influence on the rate of heat and mass transfer. It is noted that the values of the heat transfer rate are higher than that of the mass transfer whatever the value of amplitude A .

Figure 7 represents the variation of the average Nusselt and the Sherwood numbers according to the undulation number N . The evolution of these two numbers is characterized by a minimal value which corresponds to the same value of undulation $n = 3$. The maximum value of Nu_{avg} corresponds to the value $n = 2$, while the maximum value of Sh_{avg} corresponds to $n = 1$. It is also noticed that the two numbers evolve in a decreasing way with the increase of the undulation number N . The variation of N gives a rate of mass transfer increasingly higher than that of the rate of heat transfer.

Figure 8 represents the distribution of the isotherms, the streamlines and the isoconcentrations for various values of the Buoyancy ratio $N = -10, -1$ and 10 . It is observed that the distribution is carried out according to two cases:

1st case, $N < -1$: The structure of the flow is characterized by only one convective cell whose intensity of the circulation forces is more important in the fluid layer. The cell is characterized by an anticlockwise circulation and the appearance of a vortex in the vicinity of the top (hot) vertical wall. While moving away from the vertical walls of the fluid layer, the isotherms and the isoconcentrations are characterized by a heat and mass flow perpendicular to the gradient of temperature and concentration. These flows become tilted in the porous layer. The convective flow mode is more favored in the fluid layer where a high thermal and mass gradient is observed on the top part of the cavity.

2nd case, $N > -1$: It is observed that the transport phenomena is reversed and the flow structure is always characterized by only one more intense convective cell in the fluid layer which circulates in a clockwise direction. This convective cell is characterized by a vortex in the vicinity of the top of the cold vertical wall. The isoconcentrations and the isotherms are always characterized by a high heat and mass gradient in the upper part of the cavity.

In the critical case where $N = -1$ the distribution is characterized by a pure conduction and diffusion mode where the second order law of Fick is checked. The isotherms and the isoconcentrations are completely parallel to the vertical walls.

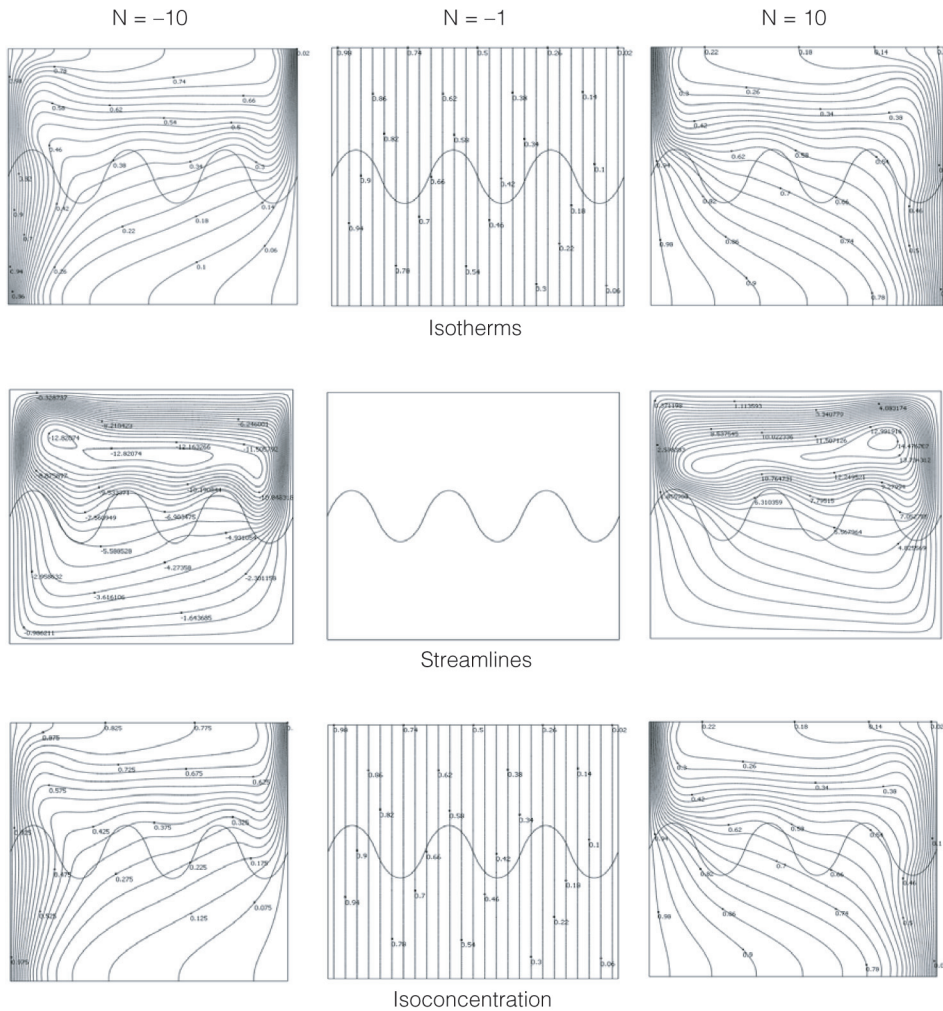


Figure 8 Isotherms Streamlines and Isoconcentration for $Ra = 10^5$; $Da = 10^{-4}$; $Le = 0,84$; $n = 3$; $Pr = 0,71$, $\epsilon = 0,5$, $A = 0,1$ and $N = 10; -1, -10$.

Figure 9 represents the variation of the Nusselt and the average Sherwood numbers according to the Buoyancy ratio N . The increase in the N decreases the heat and mass transfer until the critical point $N = -1$ where the pure conduction and diffusion appear. For Values of $N > -1$, the heat and mass transfer increase. It is also noticed that the variation of the average Nusselt number is slightly high with that of average Sherwood number, except in the case where: $-2 \leq N \leq 0$, the variation of Nu_{avg} and Sh_{avg} are almost the same.

Figure 10 represents the numerical cloud of points of the variation average Nusselt and Sherwood numbers according to the buoyancy ratio makes it possible to adopt a mathematical regression equation based on the square methods optimization.

An exponential model is selected for the case $N > -1$:

$$Nu_{avg} = 8,9 - (0,6e^{-0,8N} + 6,1e^{-0,07N})$$

$$Sh_{avg} = 8,7 - (0,65e^{-0,6N} + 6,06e^{-0,06N})$$

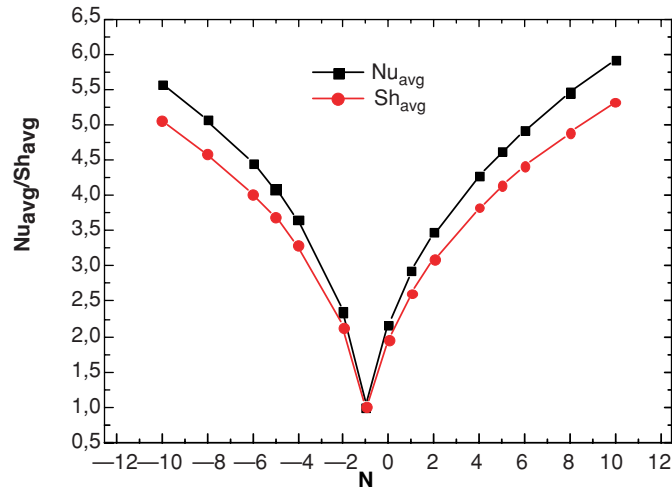


Figure 9 Average Nusselt and Sherwood number us function of N , for $Ra = 10^5$, $n = 3$, $Da = 10^{-4}$, $Le = 0.84$, $A = 0,1$, $\varepsilon = 0,5$.

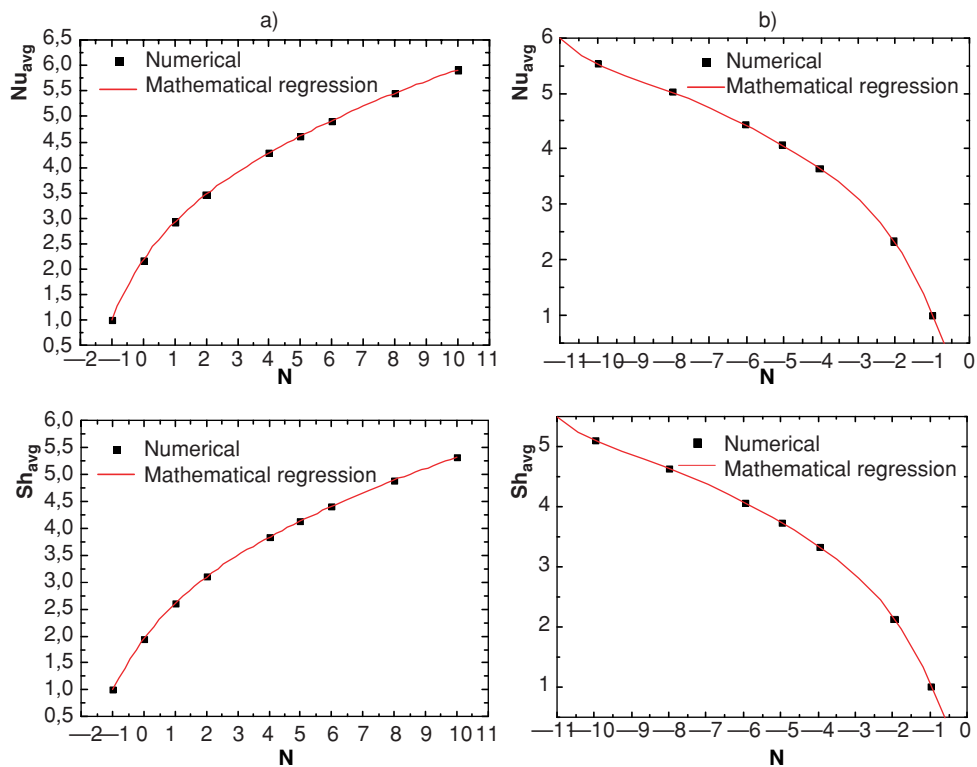


Figure 10 Evolution of the average Nusselt and Sherwood number us function for $Ra = 10^5$, $n = 3$, $Da = 10^{-4}$, $Le = 0,84$, $A = 0,1$, $\varepsilon = 0,5$ a) $N > -1$, b) $N < -1$.

For the case $N < -1$, a seven order model is selected:

$$Nu_{avg} = -(1,4 + 3,14N + 0,9N^2 + 0,14N^3 + 0,01N^4 + 3,6 \cdot 10^{-4}N^5)$$

$$Sh_{avg} = -(0,9 + 2,4N + 0,6N^2 + 0,1N^3 + 0,008N^4 + 2,4 \cdot 10^{-4}N^5)$$

The test of Student and Fischer were used to determine the significance of the parameters of the regression equations. With a confidence interval of 0,99 and a regression coefficient $R = 0,99$.

5. CONCLUSION

Using the Navier Stokes equations coupled to the Darcy Brinkman model, a numerical study, based on the finite element method, has been conducted to analyse the influences of the wavy interface parameters and the buoyancy ratio on the double diffusive natural convection occurring in a square cavity containing simultaneously a saturated horizontal porous layer and binary fluid (air + pollutant) . The following conclusions can be drawn.

- The flow is in a clockwise direction in the region of the fluid and porous layer except in the case of the effect buoyancy ratio. The cell is characterized by an anticlockwise circulation.
- The dimensionless amplitude of the wavy interface does not have any influence on the heat and mass transfers in the porous layer.
- For various values of the amplitude, the rate of heat transfer is higher than that of the mass transfer.
- The increase in the value of the amplitude widened the pseudoconductif zone of the cavity, which favoured the separation of the binary fluid.
- Increase in undulation number n , weakened the force circulation of the flow.
- The buoyancy ratio has a considerable influence on the transport phenomena and the rotation direction of the flow.
- The evolution of the average Nusselt and Sherwood numbers follows exponential and polynomial mathematical regressions with a regression coefficient $R = 0,99$.

REFERENCES

- [1] J.S. Turner, The behavior of a stable salinity gradient heated from below, *J. Fluid Mech.* 33 (1968) 183–200.
- [2] H.K. Wee, R.B. Keey, M.J. Cunningham, Heat and moisture transfer by natural convection in a rectangular cavity, *Int. J. Heat Mass Transfer* 32 (1989) 1765–1778.
- [3] F. Chen, C.F. Chen, Double-diffusive fingering convection in a porous medium, *Int. J. Heat Mass Transfer* 36 (1993) 793– 807.
- [4] O.V. Trevisan, A. Bejan, Natural convection with combined heat and mass transfer buoyancy effects in a porous medium, *Int. J. Heat Mass Transfer* 28 (1985) 1597–1611.
- [5] O.V. Trevisan, A. Bejan, Mass and heat transfer by natural convection in a vertical slot filled with porous medium, *Int. J. Heat Mass Transfer* 29 (1986) 403–415.
- [6] O.V. Trevisan, A. Bejan, Combined heat and mass transfer by natural convection in a vertical enclosure, *ASME J. Heat Transfer* 109 (1987) 104–112.
- [7] T.F. Lin, C.C. Huang, T.S. Chang, Transient binary mixture natural convection in square enclosures, *Int. J. Heat Mass Transfer* 33 (1990) 287–299.
- [8] C. Beghein, F. Haghghat, F. Allard, Numerical study of double diffusive natural convection in a square cavity, *Int. J. Heat Mass Transfer* 35 (1992) 833–846.
- [9] V.A.F. Costa, Double diffusive natural convection in a square enclosure with heat and mass diffusive walls, *Int. J. Heat Mass Transfer* 40 (1997) 4061–4071.

- [10] V.A.F. Costa, Double-diffusive natural convection in parallelogrammic enclosures filled with fluid-saturated porous media, *Int. J. Heat Mass Transfer* 47 (2004) 2699–2714.
- [11] V.A.F. Costa, Double-diffusive natural convection in parallelogrammic enclosures, *Int. J. Heat Mass Transfer* 47 (2004) 2913–2926.
- [12] A.J. Chamkha, H. Al-Naser, Double-diffusive convection in an inclined porous enclosure with opposing temperature and concentration gradients, *Int. J. Therm. Sci.* 40 (2001) 227–244.
- [13] A.J. Chamkha, Double-diffusive convection in a porous enclosure with cooperating temperature and concentration gradients and heat generation or absorption effects, *Numer. Heat Transfer, Part A* 41(2002) 65–87.
- [14] A.J. Chamkha, H. Al-Naser, Hydromagnetic double-diffusive convection in a rectangular enclosure with opposing temperature and concentration gradients, *Int. J. Heat Mass Transfer* 45 (2002) 2465–2483.
- [15] A.J. Chamkha, H. Al-Naser, Hydromagnetic double-diffusive convection in a rectangular enclosure with uniform side heat and mass fluxes and opposing temperature and concentration gradients, *Int. J. Therm. Sci.* 41 (2002) 936–948.
- [16] F.Y. Zhao, D. Liu, G.F. Tang, Application issues of the streamline, headline and massline for conjugate heat and mass transfer, *Int. J. Heat Mass Transfer* 50 (2007) 320–334.
- [17] J. Lee, M.T. Hyun, Y.S. Kang, Confined natural convection due to lateral heating in a stably stratified solution, *Int. J. Heat Mass Transfer* 33 (1990) 869–875.
- [18] J.W. Lee, J.M. Hyun, Time-dependent double diffusion in a stably stratified fluid under lateral heating, *Int. J. Heat Mass Transfer* 34 (1991) 2409–2421.
- [19] J.W. Lee, J.M. Hyun, Double-diffusive convection in a cavity under a vertical solutal gradient and a horizontal temperature gradient, *Int. J. Heat Mass Transfer* 34 (1991) 2423–2427.
- [20] T.A. Newell, J.R. Hull, Depth sounding diagnostic measurement of salt gradient solar ponds, *J. Solar Energy Eng.* 107 (1985) 160–164.
- [21] T.L. Bergman, A. Ungan, Experimental and numerical investigation of double-diffusive convection induced by a discrete heat source, *Int. J. Heat Mass Transfer* 29 (1986) 1695–1709.
- [22] W. Chen, F.Y. Zhao, G.F. Tang, D. Liu, Transportation of indoor double diffusive mixed convection coupled with diffusion in solid walls, *J. HV&AC* 36 (2006) 12–18.
- [23] F.Y. Zhao, D. Liu, G.F. Tang, Multiple steady flows in confined gaseous double diffusion with discrete thermosolutal sources, *Phys. Fluids* 19 (10) (2007) 107103.
- [24] F.Y. Zhao, D. Liu, G.F. Tang, Natural convection in a porous enclosure with a partial heating and salting element, *Int. J. Therm. Sci.* (2007), doi:10.1016/j.ijthermalsci.2007.04.006.
- [25] F.Y. Zhao, D. Liu, G.F. Tang, Free convection from one thermal and solute source in a confined porous medium, *Transport Porous Media* (2007), doi: 10.1007/s11242-007-9106-7.
- [26] D. Liu, F.Y. Zhao, G.F. Tang, Thermosolutal convection in a saturated porous enclosure with concentrated energy and solute sources, *Energy Convers. Manage.* 49 (2008) 16–31.
- [27] A. Trevisan, O.V. Bejan, Natural convection with combined heat and mass transfer buoyancy effects in a porous medium, *International Journal of Heat and Mass Transfer* 28 (1985) 1597–1611.
- [28] D. Angirasa, G.P. Peterson, I. Pop, Combined heat and mass transfer by natural convection with opposing buoyancy effects in a fluid saturated porous medium, *International Journal of Heat and Mass Transfer* 40 (1997) 2755–2773.
- [29] S. Akbal, A.F. Baytas, Numerical analysis of gas transfer by natural convection in a fluid saturated porous medium, in: R. Bennacer, A.A. Mohamad, M. El-Ganaoui, J. Sicard (Eds.), *Proc. of 4th ICCHMT: Progress in Computational Heat and Mass transfer*, 2005, pp. 313–315.
- [30] J.H. Merkin, T.Mahmood, Convective flows on reactive surfaces in porous media, *Transport in Porous Media* 33 (1998) 279–293.
- [31] B. Goyeau, D. Songbe, J.-P. Gobin, Numerical study of double-diffusive natural convection in a porous cavity using the Darcy–Brinkman formulation, *International Journal of Heat and Mass Transfer* 39 (1996) 1363–1378.

[32] A. Bahloul, L. Kalla, R. Bennacer, H. Beji, P. Vasseur, Natural convection in a vertical porous slot heated from below and with horizontal concentration gradients, *International Journal of Thermal Sciences* 43 (2004) 653–663.

[33] V.A.F. Costa, Double diffusive natural convection in a square enclosure with heat and mass diffusive walls, *International Journal of Heat Mass Transfer* 40 (1997) 4061–4071.

[34] D. Gobin, B. Goyeau, A.A. Neculae, Convective heat and solute transfer in partially porous cavities, *International Journal of Heat and Mass Transfer* 48 (2005) 1898–1908.

[35] A.K. Singh, T. Paul, G.R. Thorpe, Natural convection due to heat and mass transfer in a composite system, *Heat and Mass Transfer* 35 (1999) 39–48.

[36] L.B. Younis a, A.A. Mohamad, A.K. Mojtabi, Double diffusive convection in a vertical rectangular cavity, *International Journal of Thermal Sciences* 46 (2007) 112–117.

[37] Ohoa-Tapia, J.A., Momentum transfert at the boundary between a porous medium and a homogenous fluid-I.Theoretical developmment, *Int. J. Heat Mass Transfer* 38 (1995) 2635–2646.

[38] Goyeau, B., Lhuillier, D., Gobin, D., & Velarde, M.G. 2003. Momentum transport at a fluid-porous interface, *Int. J. Heat Mass Transfer* 46 (2003) 4071–4081.

[39] M. Mamou, P. Vasseur, E. Bilgen, Multiple solutions for double-diffusive convection in a vertical porous enclosure, *Int. J. Heat Mass Transfer* 38 (1995) 1787–1798.

[40] R. Bennacer, H. Beji, A.A. Mohamad, Double diffusive convection in a vertical enclosure inserted with two saturated porous layers confining a fluid layer, *Int. J. Thermal Science* 42 (2003) 141–151.

[41] V.A.F. Costa, L.A. Oliveria, B.R. Baliga, A.C.M. Sousa, Simulation of coupled flows in adjacent porous and open domains using a control volume finite element method, *Numerical Heat Transfer, Part A* 45 (2004) 675– 697.

[42] Beckermann, C. Ramadhyani, S., Viskanta, R., Natural convection flow and heat transfer between a fluid layer and a porous layer inside a rectangular enclosure, *J. Heat Transfer* Vol 109, pp 363-370, (1987).

[43] Sathe .S.B., Lin .W.Q et Tong. T.W., Natural convection in enclosures containing insulation with a permeable fluid-porous interface. *Int. J. Heat Fluid Flow*, vol. 9, pp 389–39, (1988).

Nomenclature

A	dimensionless amplitude, a/L	U, V	nondimensional velocity components
a	amplitude m	x, y	Cartesian coordinates
C	species concentration kgm^{-3}	X, Y	nondimensional coordinates
D	mass diffusivity m^2s^{-1}	Greek symbols	
Da	Darcy number	α	thermal diffusivity m^2s^{-1}
k	thermal diffusivity	β_T	coefficient of thermal expansion K^{-1}
K	permeability of the porous layer m^2	β_c	coefficient of concentration expansion m^3kg^{-1}
L	height of square porous cavity . . . m	ν	fluid kinematic viscosity m^2s^{-1}
Le	Lewis number	θ	dimensionless temperature
N	buoyancy ratio	ρ	fluid density kg m^{-3}
Nu_{avg}	average Nusselt number	τ	nondimensional time
Nu_L	local Nusselt number	ϵ	porosity
P	pressure Nm^{-2}	Subscripts	
Pr	Prandtl number	f	fluid
Ra	thermal Rayleigh number	p	porous
Sh_{avg}	average Sherwood number	eff	effective
Sh_L	local Sherwood number	L	left
τ^*	time s	R	right
T	temperature K	*	Dimensional properties
U^*	velocity components along x . . ms^{-1}	C	cold and H hot
V^*	velocity components along y . . ms^{-1}		